

ANGULAR NEUTRON FLUX MEASUREMENTS AND NUCLEAR DATA TEST
ON SLABS OF FUSION BLANKET MATERIALS

Yukio Oyama, Kazuaki Kosako, Seiya Yamaguchi and Hiroshi Maekawa

Japan Atomic Energy Research Institute
Tokai-mura, Naka-gun, Ibaraki-ken 319-11, Japan

Abstract: Angular neutron flux spectra leaking from slab assemblies of Li, Be, C and Li₂O with irradiation of DT neutrons have been analyzed to test the nuclear data in JENDL-3T through comparison with the experimental results. The energy spectra were measured in the range of 15 MeV down to 80 keV using the time-of-flight method with an NE213 liquid scintillator. The slab thicknesses were 0.5 to 5 mean free path for 14.8 MeV neutrons. The experiment were analyzed by the Monte Carlo codes, MCNP and MORSE-DD with various nuclear data files. The nuclear data in JENDL-3T show better agreements with the experiments except for beryllium.

(Angular Neutron Flux, TOF, Fusion Blanket, JENDL-3T, Lithium, Beryllium, Carbon, Lithium- Oxide, MCNP, MORSE-DD)

Introduction

New evaluation of nuclear data on light nuclei had been performed as JENDL-3T^{*1} for a fusion reactor design application. The evaluation was based on the recent measurements of double differential cross sections^{2,3}. In order to examine the validity of the nuclear data in JENDL-3T, an test by comparison with the experiments is required for practical bulk systems relevant to the fusion reactor.

On fusion blanket materials, angular flux measurements had been carried out for DT neutrons using the time-of-flight method⁴⁻⁶. The angular neutron flux spectrum leaked from a slab is a basic quantity to calculate the neutronic parameters and provides directly the bulk effect of neutron transport. The measurements were performed systematically with neutron leaking angle and slab thickness.

In the present paper, nuclear data on Li, Be, C and Li₂O in JENDL-3T have been tested through comparison between the angular flux measurements and the Monte Carlo calculations. For thin slab, the spectrum reflects directly double differential cross sections. On the other hand, from thickness dependence, the nuclear data can be examined with neutron transport characteristics. Hence, we can discuss the overall sufficiency of the nuclear data for a practical application.

ExperimentAngular Flux Measurement

The measurement of neutron angular flux spectra on a slab was carried out by the time-of-flight method with an 50.8 mm dia. and 50.8 mm long NE213 scintillation detector. The neutron energy spectrum was obtained in the range of 0.08 MeV to 15 MeV using the two-bias scheme³ which combined two measurement runs with the different biases at the same time. The neutrons leaking from the slab were collimated on the rear surface of slab for the detector and reduced to the angular flux. The effective measured area on the slab defined by the detector-collimator system was determined from the calculated response function of leaking neutrons for the detector.

The experimental arrangement is shown in

* JENDL-3T is a temporary file for testing the evaluated data which are for JENDL-3. The data in JENDL-3T will be partly revised in JENDL-3.

Fig.1. The measured spectrum was reduced to the following quantity.

$$\phi(\Omega, E) = \frac{C(E)}{\epsilon(E) \cdot \Delta\Omega \cdot A_s \cdot S_n \cdot T(E)} \quad (1)$$

[n/sr/m²/unit lethargy/source neutron],

where

- C(E) = counts per unit lethargy for neutrons of energy E,
- $\epsilon(E)$ = neutron detector efficiency at energy E,
- $\Delta\Omega$ = solid angle subtended by the detector to the point on the surface center of the assembly, i.e., $\Delta\Omega = A_d/L^2$, where A_d = counting area of the detector and L = distance from the rear surface to the detector,
- A_s = effective measured area defined by the detector-collimator system on the plane perpendicular to the axis at the assembly surface,
- S_n = total source neutrons obtained by the associated alpha-particle monitor,
- T(E) = attenuation due to air through neutron flight.

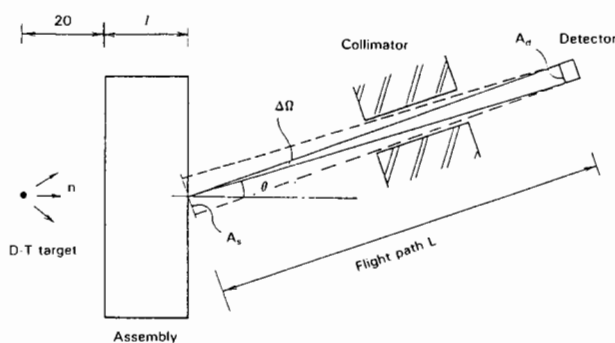


Fig.1 Experimental Arrangement

The measuring angles of emitted neutrons were selected in 0, 12.2, 24.9, 41.8 and 66.8 degrees by rotation of the detector-collimator deck.

Slab Assembly

Experimental assembly was made up in a pseudo-cylindrical slab shape of 314 mm in diameter by stacking rectangular blocks with a unit of 50.6 mm cubic. The assembly was supported by thin-walled, square aluminum tubes and placed at the distance of 200 mm from the DT neutron source at the FNS (Fusion Neutronics Source) facility in JAERI. The measured materials are of

Table 1. Experimental Assemblies used for Nuclear Data Test

Material	Assembly thickness	
Li*	100, 300 mm	(0.6-1.8 mfp)
Be	50.8, 152.4 mm	(0.9-2.7 mfp)
C	50.6, 202.4, 404.8 mm	(0.6-4.8 mfp)
Li ₂ O*	48, 200, 400 mm	(0.6-5.0 mfp)

* contained by stainless steel sheet

Li, Be, C and Li₂O, and the slab thicknesses are of 0.6 to 5 mfp (mean free path) for 14.8 MeV neutrons as listed in Table 1. The Li and Li₂O blocks were contained by stainless steel sheet to protect them from humidity and oxidization.

Monte Carlo Calculation

The Monte Carlo calculations for the experiment were performed by the continuous energy code MCNP⁷ for the Li, C and Li₂O and the multi-group code MORSE-DD⁸ for the Be. The MCNP library is FSXLIB⁹ processed by the NJOY code¹⁰ and the MORSE-DD library is DDXJ3T in a double-differential-cross-section form of 125 groups processed by PROF-DD¹¹.

The point detector estimator was used in the both calculations. The MCNP calculations were done simultaneously for five angles. The collimator was simulated by cylindrical regions with an opening area A_s . The outside of the cylinders was assigned to no-importance region in which neutron history was immediately terminated.

The calculational model for the MORSE-DD calculations is shown in Fig.2. The neutrons within a solid angle of $\Delta\Omega'$ are accounted, and then by using a relation of $\Delta\Omega' = A_s/L^2$ and $\Delta\Omega = A_d/L^2$, we obtain the flux equivalent to the measured one.

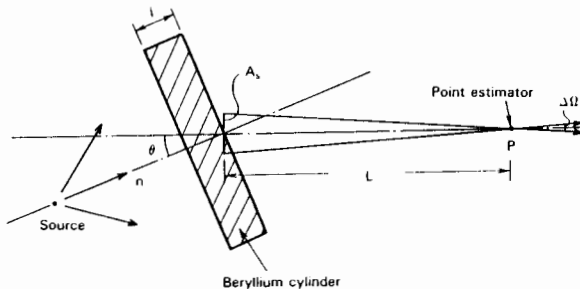


Fig.2 Model for MORSE-DD calculation

Results and Discussions

Carbon

The nuclear data of JENDL-3T for carbon is the same as those of JENDL-3PR2.¹² The differences between the data of JENDL-3PR1¹² and -3PR2(3T) are only for the higher elastic and lower third inelastic cross sections for 14.8 MeV neutrons. Total and elastic cross sections of JENDLs are a few % lower than the ENDF/B-V.

The measured and calculated spectra are shown in Fig.3. The results by both JENDLs show almost the same spectra, except for small differences in the peaks of second and third inelastic levels. To examine the differences in detail, the flux

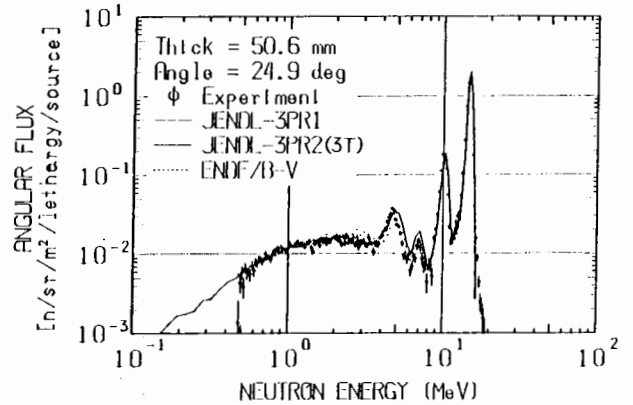


Fig.3 Measured and calculated spectra for the graphite slab

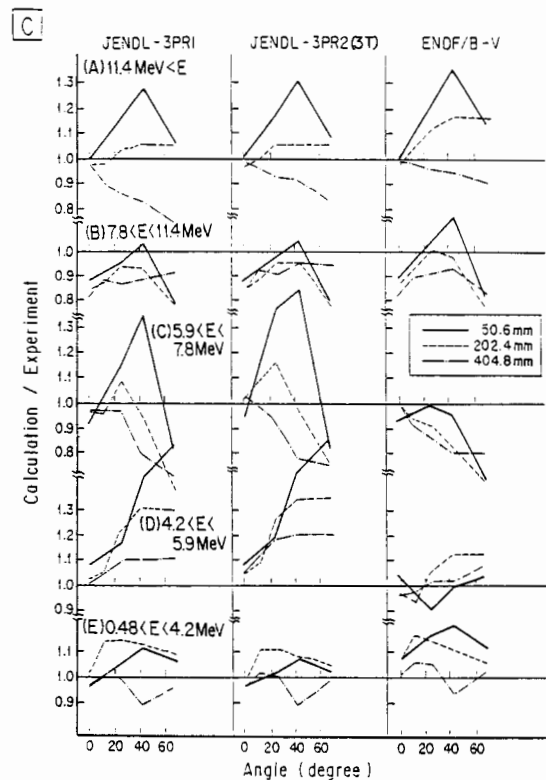


Fig.4 Comparison of the calculated-to-measured value (C/E) ratio for the energy region-wise flux for the graphite slab

integrated over the interest energy regions were compared in the form of the calculated-to-measured value (C/E) ratio as shown in Fig.4.

From the 50.8 mm case, it can be pointed out that: (1) Three files overestimate the elastic reaction neutrons by 30 % at 40 degrees, and (2) For inelastic scatterings by the 7.65 and 9.64 MeV levels, the JENDLs overestimate the flux by 40 % at large angle.

From thickness dependence, we can see the overall trend of the nuclear data validity through neutron penetration. In the elastic reaction neutron region, the three files show different trends with thickness increase, i.e., the higher elastic cross section of ENDF/B-V is better than the JENDLs for 404.8 mm case. In the regions (C) and (D), the deviations of the JENDLs decrease

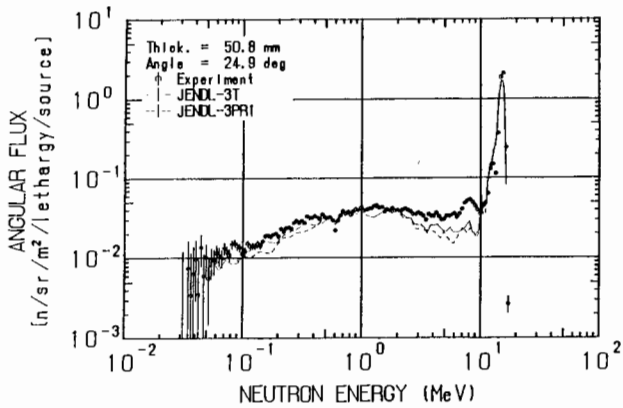


Fig. 5 Measured and calculated spectra for the beryllium slab

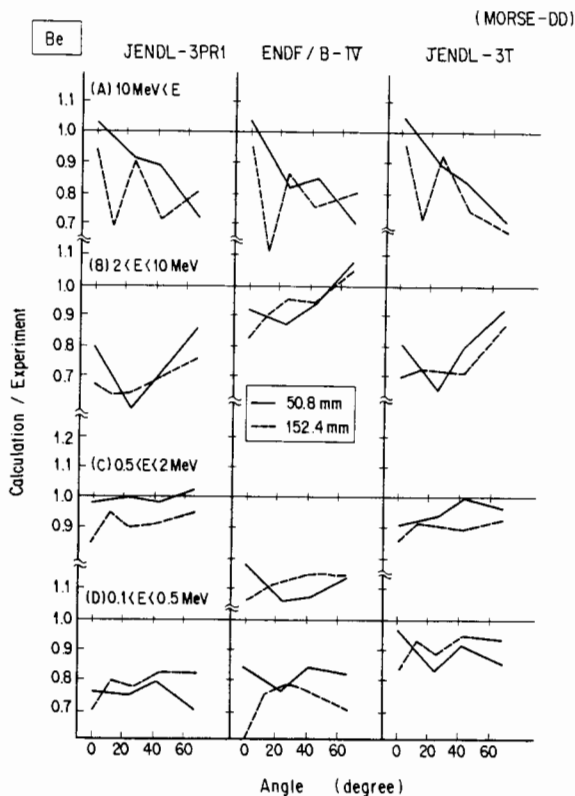


Fig. 6 Comparison of the calculated-to-measured value (C/E) ratio for the energy region-wise flux for the beryllium slab

with thickness increase. This is ascribed to neutrons scattered down from higher energy regions, i.e., the initially scattered neutrons of low energy are buried in the neutrons down-scattered by elastic reaction.

Beryllium

The beryllium data of JENDL-3T is 3 % lower for the elastic cross section and 10 % higher for the inelastic cross sections than those of JENDL-3PR1, and is different for a level configuration of (n,2n) reaction from the ENDF/B-IV.

The comparison of the calculated spectra with the experiment is shown in Fig.5. There is a large discrepancy with the measurement in the 2-10 MeV range for both calculations of JENDLs. The C/E ratio of the integrated flux is shown in Fig.6. In the figure, the both JENDL calculations also underestimate the flux by 30 % in the range of 2-10 MeV. This is not caused by angular dependence

of inelastic scattering but by the inelastic total cross section. However, the JENDL-3T show better agreements for low energy region than the JENDL-3PR1 because of the higher inelastic cross sections of JENDL-3T. The three calculations above 10 MeV underestimate the flux at the large angle. This suggests that the data of angular dependence of the elastic cross section or the total scattering cross section for 14.8 MeV neutrons should be re-examined.

Lithium and Lithium-Oxide

The ⁷Li nuclear data of JENDL-3T is 9 % higher for the inelastic cross sections of high order levels than those of JENDL-3PR1 and -3PR2. The angular distributions of neutrons scattered by 4.63 MeV level are improved for JENDL-3T and -3PR1. The oxygen data of JENDL-3T is 6 % lower for the elastic cross section and 6 % higher for the inelastic cross sections than the JENDL-3PR1.

The spectra for the lithium and lithium-oxide assemblies are shown in Figs.7 and 8, respectively. The agreement of both calculations with the experiment is very good. The small discrepancies are seen at the peak of the 4.63 MeV level scattering and below 300 keV. The discrepancy in the low energy, however, becomes smaller with increasing the thickness.

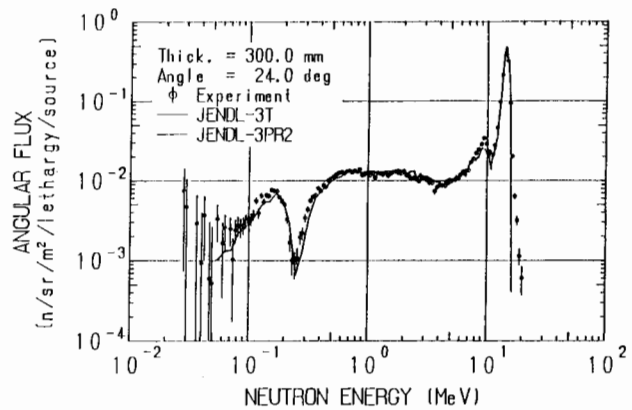


Fig. 7 Measured and calculated spectra for the lithium slab

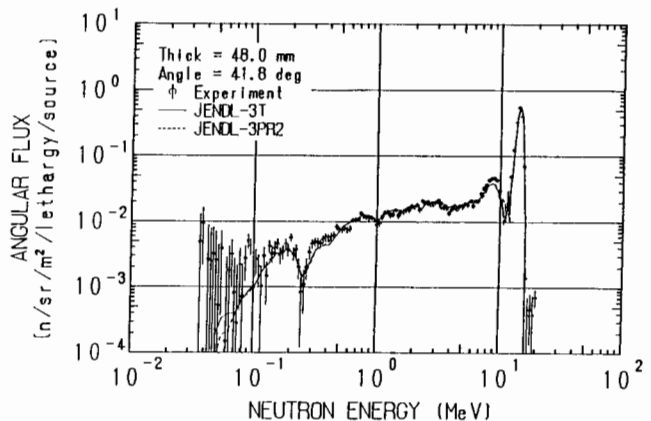


Fig. 8 Measured and calculated spectra for the lithium-oxide

The C/E comparison for the lithium-oxide assembly is also shown in Fig.9. In the figure, the JENDL-3T and -3PR2 show excellent agreements with the measurement within 10 % for all energy regions and angles. The JENDL-3PR2 and -3T were improved for the region (E) from the thickness dependence. However, it is suggested that the total cross section of ^7Li in JENDL-3T is slightly small, since the 0 degree flux are largely changed, while the JENDL-3PR1 is not changed much.

Figure 10 show the case when the oxygen data alone is changed from JENDL-3PR1 to -3T. The results of the C/E ratios are almost the same as the JENDL-3T, though the cross sections of oxygen are largely changed by $\sim 6\%$.

Summary

From the present comparisons, it is pointed out for application of JENDL-3T to a fusion neutronics calculation that:

- 1) Carbon data overestimate the neutrons scattered by the second and third level inelastic cross section, but after penetration over 2 mfp, the predicted spectra become good.
- 2) Beryllium data underestimate the flux of 2-10 MeV. This may cause the underprediction of tritium production rate from ^7Li in beryllium contained blanket.
- 3) Lithium data is sufficient at present, but it is necessary to check the total cross section.
- 4) Selection of oxygen data, JENDL-3T or -3PR1, is not affective in the lithium-oxide assembly. The present data is sufficient.

References

1. JENDL Compilation Group (Nuclear Data Center, JAERI), JENDL-3T, private communication (1987)
2. A. Takahashi, et al., J. Nucl. Sci. Technol., 21[8], 577 (1984)
3. S. Chiba, et al., *ibid.*, 22[10], 771 (1985)
4. Y. Oyama and H. Maekawa, Nucl. Instr. Method, A245, 173 (1986)
5. *idem.*, Nucl. Sci. Eng., 97, 220 (1987)
6. Y. Oyama, et al., J. Nucl. Sci. Technol., 25[5], 419 (1988)
7. Los Alamos Radiation Transport Group (X-6), LA-7396-M (1981)
8. M. Nakagawa and T. Mori, JAERI-M 84-126 (1984).
9. K. Kosako, et al., JAERI-M 88-076 (1988) (In Japanese)
10. R. E. MacFarlane, et al., LA-9303-M (1982)
11. T. Mori, et al., JAERI-M 86-124 (1986)
12. K. Shibata and Y. Kikuchi, "Evaluation of Nuclear Data for Fusion Neutronics," Proc. Int. Conf. Nuclear Data for Basic and Applied Science, Santa Fe, p. 1985 (1986)

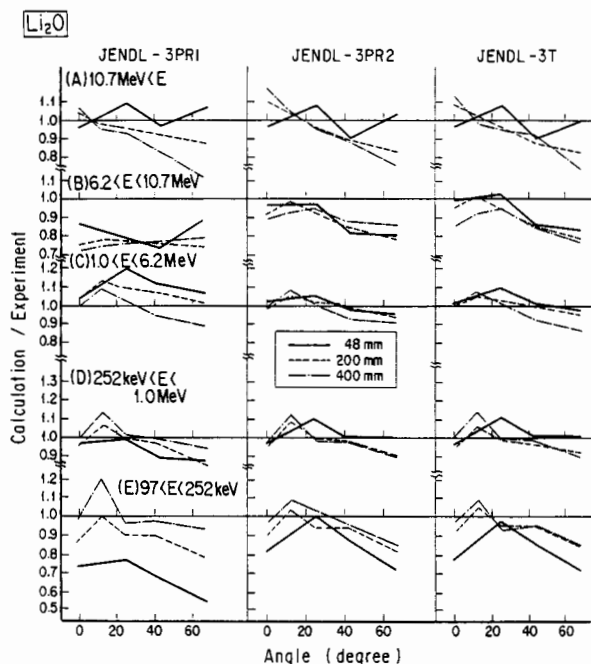


Fig.9 Comparison of the calculated-to-measured value (C/E) ratio for the energy region-wise flux for the lithium-oxide slab

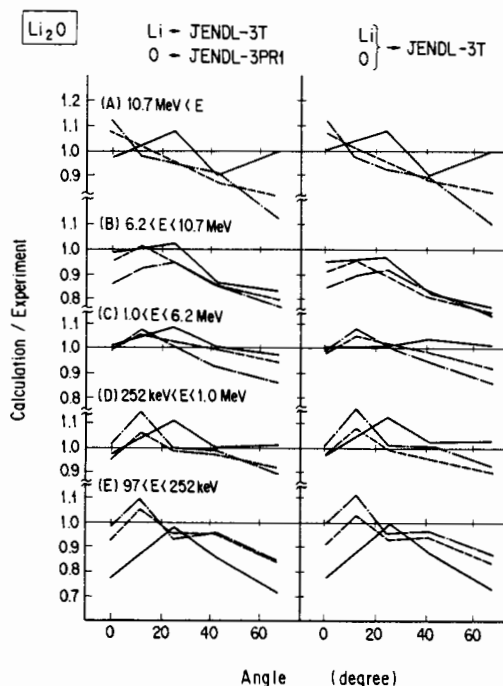


Fig.10 Effect of oxygen data change on the C/E ratios for the lithium-oxide slab